Journal of Membrane Science 369 (2011) 284–289

Contents lists available at ScienceDirect

Journal of Membrane Science

journal homepage: www.elsevier.com/locate/memsci

Ethene/ethane separation by the MOF membrane ZIF-8: Molecular correlation of permeation, adsorption, diffusion

Helge Bux[a], Christian Chmelik[b], Rajamani Krishna[c], Juergen Caro[a,*]

[a] Institute of Physical Chemistry and Electrochemistry, Leibniz University Hannover, Callinstr. 3A, D-30167 Hannover, Germany
[b] Faculty of Physics and Geosciences, Leipzig University, Linnéstr. 5, D-04103 Leipzig, Germany
[c] Van't Hoff Institute for Molecular Sciences, University of Amsterdam, Science Park 904, 1098 XH, Amsterdam, The Netherlands

ARTICLE INFO

Article history:
Received 27 September 2010
Received in revised form
29 November 2010
Accepted 2 December 2010
Available online 8 December 2010

Keywords:
MOF membrane
ZIF-8 membrane
Ethene/ethane separation
IR microscopy
GCMC simulations

ABSTRACT

The newly developed MOF membrane ZIF-8 separates an equimolar ethene/ethane mixture at room temperature for 1 and 6 bar feed pressure, respectively, with a selectivity of 2.8 and 2.4. Independent sorption uptake studies of an ethene/ethane mixture on a big ZIF-8 single crystal by IR microscopy detection show in combination with grand canonical Monte Carlo simulations that this moderate ethene selectivity of the ZIF-8 membrane can be explained by the interplay of a preferential ethane adsorption selectivity competing with a preferential ethene diffusion selectivity. This means, that ethane adsorbs stronger than ethene, but ethene diffuses faster and overcompensates the adsorption preference of ethane, resulting in a membrane permeation selectivity for ethene.

1. Introduction

The paraffin/olefin separation by cryogenic distillation is one of the most energy and cost intensive processes. Separation by adsorption is an energy-efficient alternative. Two concepts can be applied: (i) the preferential uptake of the olefin under equilibrium condition e.g. by Cu modified adsorbents and (ii) the kinetic based separation by different diffusion rates, which result in the extreme case to steric size exclusion.

As a new type of nanoporous materials, metal–organic frameworks (MOFs) have been examined inter alia in their olefin/paraffin separation performance by adsorption [1]. By chlorine or bromine functionalization of organic linker molecules, the pore openings of zeolitic imidazolate frameworks (ZIFs) could be fine-tuned. The modification resulted in different diffusion rates – propene is slightly smaller and hence is diffusing faster than propane – and allowed kinetic separation of the mixture [2]. In contrary, copper containing MOFs like $Cu_3(BTC)_2$ showed favored adsorption of i-butene above i-butane, allowing the separation of the binary mixture in packed bed adsorber [3]. For liquid C_5 paraffin/olefin mixtures, $Cu_3(BTC)_2$ shows a clear olefin selectivity as well [4].

Very recently, first MOF membranes with selectivities higher than the Knudsen selectivity have been developed [5–12]. In our recent works, we focused on the development of thermally stable and steam resistant ZIF membranes like ZIF-7 [13–15], ZIF-8 [16] and ZIF-22 [17]. Despite pioneering works in the field of computer modeling to predict separation behavior of MOF adsorbents [18] and membranes [19], the experimental separation factors often differ considerably from the predictions [20]. These deviations might be correlated to the framework flexibility of the MOFs.

The in situ study of sorption uptake/desorption of guest molecules on large MOF or zeolite crystals detected by IR microscopy (IRM) supported by theoretical studies by grand canonical Monte Carlo (GCMC) simulations appears to be a powerful tool for determining loading dependent transport diffusion coefficients under mixed gas conditions [20,21]. Using the well-known relationship "permeability = mobility × solubility" as a rough estimation, the membrane selectivity can be expressed as the product of a diffusion and adsorption selectivity [22]. Here, we study ethene/ethane separation on a supported ZIF-8 membrane and give a molecular interpretation of the adsorption and diffusion contributions from GCMC supported IRM (GCMC-IRM) studies on large ZIF-8 single crystals.

2. Experimental

As recently reported, continuous ZIF-8 layers can be grown as membrane on-top of porous titania supports [16]. However, the

* Corresponding author.
E-mail addresses: juergen.caro@pci.uni-hannover.de, caro@pci.uni-hannover.de (J. Caro).

0376-7388/$ – see front matter © 2010 Elsevier B.V. All rights reserved.
doi:10.1016/j.memsci.2010.12.001

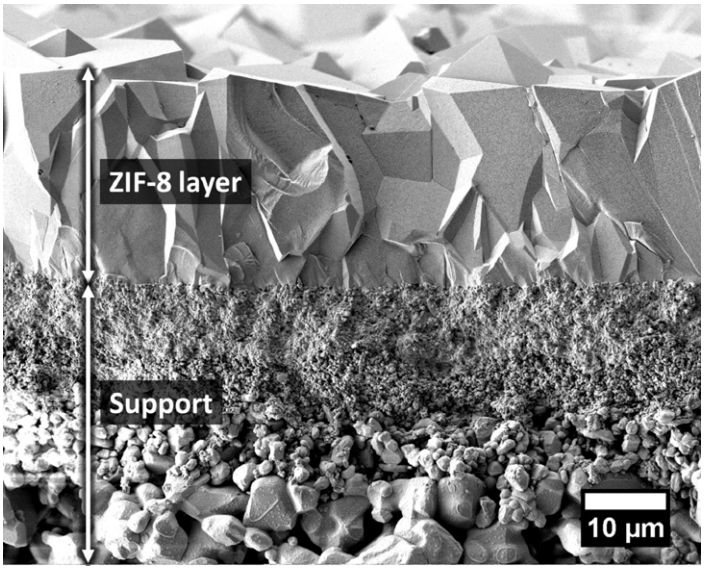

Fig. 1. Cross-section of the supported ZIF-8 membrane.

discoid titania supports of 1 mm thickness turned out to be too brittle for application at pressures difference across the membrane >3 bar. Hence, in this work a special composite support (Fraunhofer IKTS, Germany) consisting of a smooth titania layer on top of a mechanically strong alumina support was used for membrane preparation.

A typical synthesis solution contains 0.538 g (3.95 mmol) zinc chloride (>99% Merck), 0.486 g (5.92 mmol) 2-methylimidazole (>99%, Sigma–Aldrich) and 0.268 g (3.95 mmol) sodium formate (>99%, Sigma–Aldrich) solved by ultrasonic treatment in 80 ml methanol (99.9%, Roth). The solution together with the calcinated support was heated in a microwave oven for 4 h at 100 °C forming ZIF-8 with the sum formula $Zn^{2+}(mim^{-})_2$ (mim^{-} = 2-methylimidazolate). After synthesis the ZIF-8 membrane was cleaned with methanol and dried at room temperature overnight. For permeation measurements the membrane as shown in Fig. 1 is mounted in a permeation cell (cf. [16]).

Permeation measurements were carried out with two different methods. Pressure dependent permeation of an equimolar ethene/ethane gas mixture was measured by the Wicke–Kallenbach technique, permeate below the membrane was carried by a sweep gas to a gas chromatograph (HP Agilent 6890N with thermal conductivity detector), equipped with a HayeSep C packed column (15 ft. 1/8 in.). In addition, pure component permeation measurements were carried out at fixed feed pressure of 6 bar and atmospheric pressure (1 bar) on the permeate feed. The single gas permeation was performed without sweep gas and the flow rate was measured by bubble counter. Ideal and mixture separation factors were calculated following IUPAC definitions [23].

By IRM the time-resolved sorption uptake of the single gases and of the components of the binary mixture on a large ZIF-8 single crystal as shown in Fig. 3 is studied. The large ZIF-8 single crystals were grown similarly like the ZIF-8 membrane with the same stoichiometric ratio of the starting chemicals but using diffusion-controlled mixing of the chemicals. Zinc chloride and 2-methylimidazole dissolved in methanol were given into an autoclave. Sodium formate in methanol, however, was contained in a PTFE container inside this autoclave. Both solutions were able to counter-diffuse through an opening in the PTFE container of ~1 cm^2. After heating the autoclave to 140 °C for 24 h in an air conditioned oven, large crystals could be collected from the inner of the PFTE container.

The gas uptake by the crystal is realized by only small step-changes of the gas phase to reduce the loading dependency of the diffusivity. The loading steps were less than 5% of the total loading for this temperature and, therefore, a constant diffusivity can be assumed for this "differential loading step". By fitting the sorption uptake curves with appropriate solutions of Fick's second law (spherical geometry, constant diffusivity, constant boundary conditions as given by Crank [24]), diffusion coefficients of ethane and ethene as pure component as well as in the mixture could be derived. The sorption uptake/desorption curves represent the relative loading averaged over the whole crystal under study as a function of time (for details see Refs. [20,21]). Furthermore, when measuring the time and space resolved IR absorbance, IRM provides the concentration profiles during ad/desorption as additional information. From these profiles (not shown here) we could state that sorption uptake/desorption is controlled by intracrystalline diffusion and not by surface barriers. The diffusivities thus determined without any corrections are called "transport diffusion coefficients D_T" (D_T in Figs. 5 and 6). IRM makes it possible to distinguish the relative amounts of the adsorbed ethene and ethane as pure component as well as in mixture. Therefore, IRM allows the determination of transient adsorption and diffusion data for the components of a mixture. Using IRM, isotherms from individual crystals were obtained in relative units of the absorbance, and additional data are necessary for calibration in order to convert the arbitrary absorbance units into absolute amounts of adsorbed molecules. GCMC simulations have proven to be an accurate tool [25–27] for the prediction of adsorption isotherms. Very recently, we have shown GCMC data for ZIF-8 including pure component ethane and ethene [20]. For the calibration of IRM this GCMC data was used, by scaling the loading axis of the IRM sorption isotherm to the best visual fit with the GCMC sorption data.

3. Results and discussion

For the correlation of the permeation selectivity with the GCMC-IRM diffusion and adsorption data, it has to be ensured that only the ZIF-8 layer on-top of the macroporous support controls the permeation. Hence, a relative thick ZIF-8 layer of about 25 μm has been prepared on top of the asymmetric titania support (Fig. 1). However, it should be noted that using secondary growth crystallization, ZIF-8 membrane layers with a few μm in thickness can be realized [13].

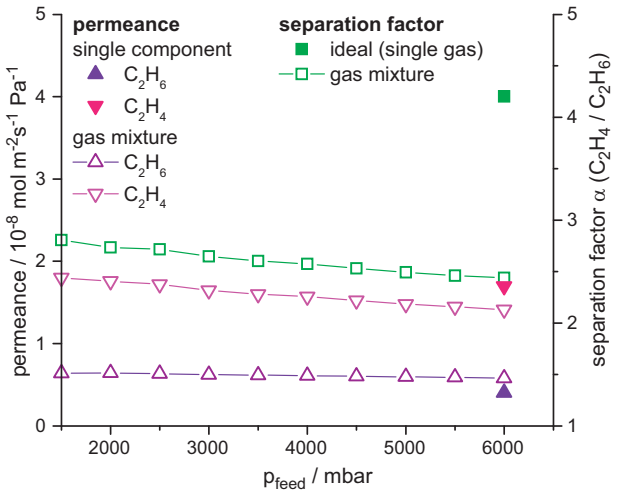

Fig. 2. Permeances and separation factors at $T = 298$ K of the ZIF-8 membrane as shown in Fig. 1 for ethene and ethane as pure component as well as in equimolar mixture for different feed pressures. The mixture measurements were carried out by the Wicke–Kallenbach technique (partial pressure of the C_2 component ≈0 at the permeate side) while for the single gas measurement no sweep gas was used (partial pressure of the C_2 component ≈1 bar at the permeate side). For gas mixtures, the permeances were calculated at $T = 293.15$ K and $p = 1.013$ bar from the applied partial pressure difference (for equimolar composition this is 1/2 feed pressure) and for pure component from the total pressure difference ($\Delta p = 5$ bar).

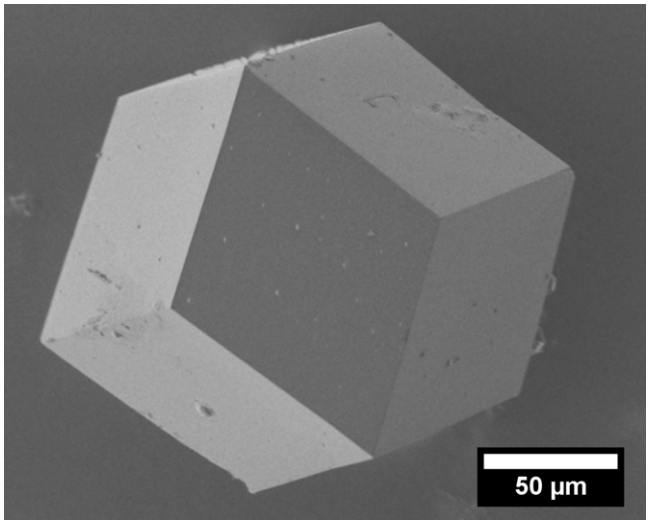

Fig. 3. Large ZIF-8 crystal with typical rhombic dodecahedral shape as used for IRM uptake/desorption measurements.

Table 1
Extended dual-site Langmuir model and parameters for ethene and ethane single gas isotherms (units: p in mbar, q in molecules/cage).

Equation	$q = A\frac{k_1 \cdot p^x}{1+k_1 \cdot p^x} + B\frac{k_2 \cdot p}{1+k_2 \cdot p}$
Parameter ethene	$A = 9$, $B = 3$, $k_1 = 1.93004 \times 10^{-4}$, $k_2 = 1.95071 \times 10^{-6}$, $x = 1.1100$
Parameter ethane	$A = 8$, $B = 3$, $k_1 = 4.46609 \times 10^{-4}$, $k_2 = 8.40412 \times 10^{-6}$, $x = 1.1231$

Fig. 2 shows the pressure dependency of the ethene/ethane separation factor α for the equimolar gas mixture measured by the Wicke–Kallenbach technique. A slight decrease in α from 2.8 to 2.4 with increasing feed gas pressure can be observed. In addition, from the pure component permeation measurements without sweep gas, an ideal separation factor of 4.2 as the ratio of the ethene flux (1.24 ml cm^{-2} min^{-1}) and the ethane flux (0.29 ml cm^{-2} min^{-1}) can be calculated. There are various reasons for the difference in separation efficiency between the pure component measurements and the mixed gas ones. First of all, both experiments were carried out under different conditions. Although for both experiments a total feed pressure of 6 bar was applied, for the mixture each gas only has a partial pressure of 3 bar. In the linear Henry region of the adsorption isotherm, equal pressure differences Δp result in equal concentration differences Δc in Fick's first law. Hence, in the Henry region experiments with and without sweep gas are generally comparable when Δp is equal. However, in our case both experiments were carried out significantly beyond this region. Hence, a direct relation of both experiments is not valid, since for both cases different Δc were present. In addition, the interplay of adsorption and diffusion effects such as mutual pore blocking as well as guest–guest interactions can highly influence the separation efficiency of gas mixtures in relation to the pure components.

The ethene selectivity of the ZIF-8 membrane can be understood in detail on the basis of the independent GCMC-IRM studies on a large ZIF-8 single crystal (Fig. 3). As shown in Fig. 4a, the pressure dependence of the amount adsorbed is captured well by both GCMC and IRM and, therefore, the adsorption data coincide, which make it possible to combine both techniques as explained in Section 2. Fig. 4b–d shows the increase in loading with increasing gas phase pressure for both single and mixed gas adsorption. Fig. 4b and c shows for the ethene/ethane mixtures of the compositions 1.9:1 and 1:1.5, that the mixture adsorption can be described very well by the ideal adsorption solution theory (IAST) [28]. The IAST data were calculated from an extended dual-site Langmuir fit of the single gas isotherms, the corresponding equation and parameters can be found in Table 1.

Although hard to see in pure component isotherms, ethane is notably stronger adsorbed compared to ethene. In mixture adsorption, the favored adsorption of ethane above ethene is much more obvious. For the ethene-rich mixture (ethene:ethane = 1.9:1) equal amounts of ethene and ethane are found in the adsorbed phase. For the ethene-poor mixture (ethene:ethane = 1:1.5) remarkably higher amounts of ethane are adsorbed. At first this finding of the preferential ethane adsorption in comparison with the ethene one seems surprising. However, for cation-free non-polar pore systems without specific interactions a thermodynamic selectivity for the adsorption of ethane over ethene is a common experimental finding[1] [29–31]. Whereas for the pure components, the amount of adsorbed ethane is only 5–10% higher than that of ethene (cf. Fig. 4a), for ethane-rich mixtures ethane is enriched by the factor of two in the adsorbed phase (cf. Fig. 4b). We cannot explain this experimental finding because of the quite similar Lennard–Jones parameters. Fig. 4d shows for the equimolar ethene/ethane mixture that the amount of adsorbed ethane is almost twice that of ethene. The pressure dependent adsorption selectivity can be obtained from the IAST model of an equimolar ethene/ethane mixture by the ratio of the adsorbed concentrations. For example, at a total pressure of 6 bar, 4.6 molecules ethane and 2.5 molecules ethene are adsorbed per cavity, giving a total loading of 7.1 C_2 molecules/cage and an ethene/ethane adsorption selectivity of around 0.5.

Fig. 5 shows the loading dependent transport diffusion coefficients D_T as obtained from the ethene and ethane sorption uptake curves from their binary mixtures. Atleast in the measured pressure range, ethene and ethane diffusivities are independent of the molar compositions of the gas mixtures i.e. the diffusivities for ethene and ethane from the mixtures of the ethene/ethane com-

[1] In a recent paper on ethane and ethane adsorption on ZIF-7, the preferred ethane adsorption is explained by a gate-opening mechanism [41].

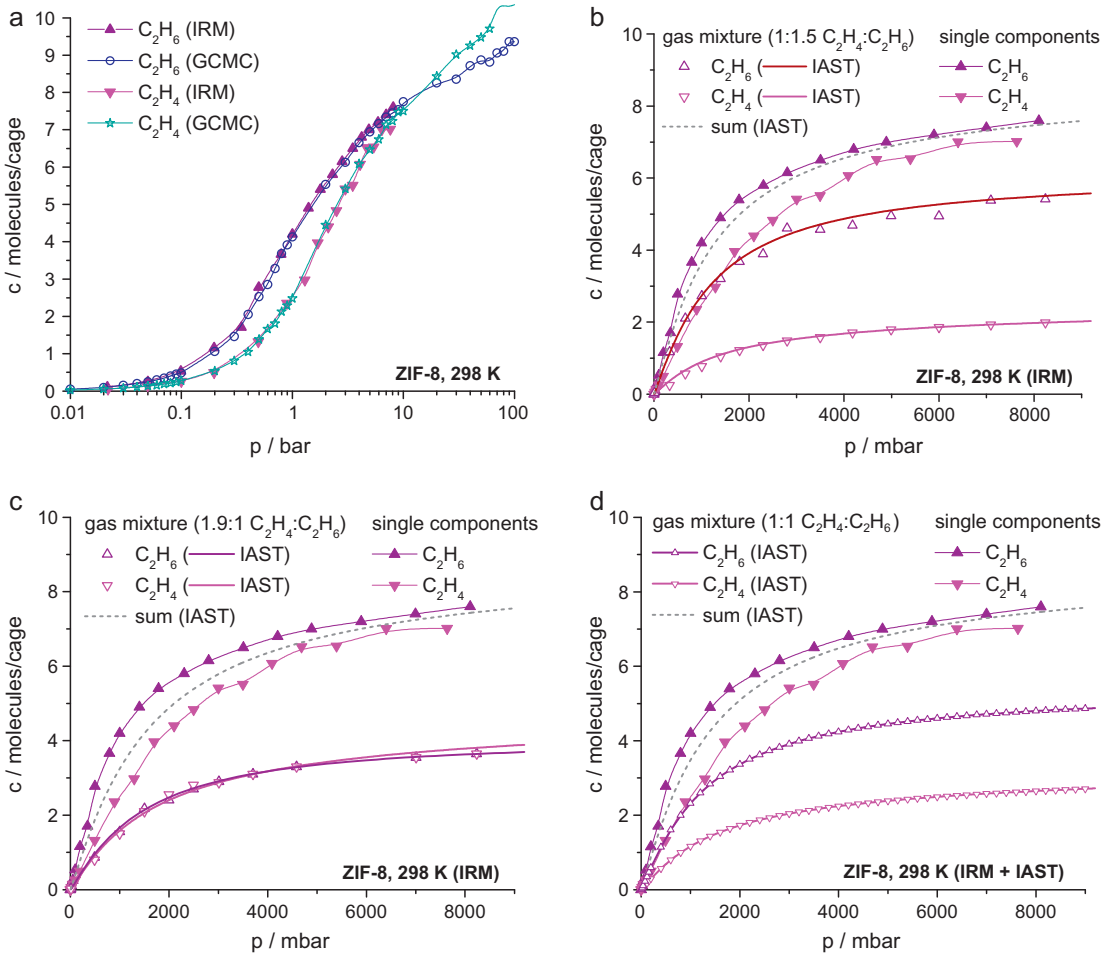

Fig. 4. (a) Ethene and ethane isotherms from pure component sorption uptake studies on a large ZIF-8 single crystal as shown in Fig. 3 were recorded by IRM at room temperature and calibrated by GCMC isotherms. (b and c) The GCMC-IRM mixture isotherms are compared with the partial ethene and ethane loadings for mixture adsorption computed by IAST (full lines). Composition of the ethene/ethane mixtures: 1:1.5 (b) and 1.9:1 (c). (d) The single gas adsorption data and the calculated partial loadings for a 1:1 ethene/ethane mixture as derived from IAST.

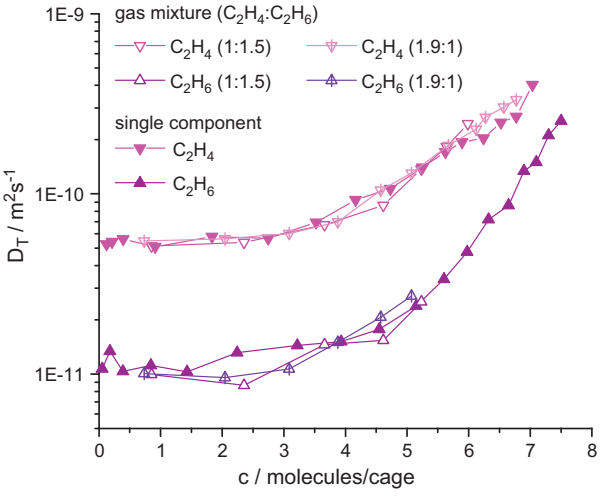

Fig. 5. Transport diffusion coefficients D_T at $T = 298$ K of ethene and ethane from mixed gas sorption uptake experiments as derived from IRM on a big single crystal as shown in Fig. 3 for two ethene/ethane compositions of the gas mixture: 1:1.5 and 1.9:1 as function of total C_2 loading (sum of ethene + ethane molecules/cage). Calibration of the IRM by GCMC.

positions 1.9:1 and 1:1.5 coincide. In particular at low loadings, ethene diffuses around 5 times faster than ethane. However, with increasing loading ethane becomes more mobile. At a loading of 7.1 C_2 molecules/cage (partial loadings of 2.5 ethene and 4.6 ethane molecules/cage), the transport diffusion coefficient of ethene is found to be 2.7 times higher than that one of the ethane. Multiplying the ethene/ethane adsorption selectivity (0.5) and diffusion selectivity (2.7), a total membrane selectivity of 1.4 is predicted for the ethene/ethane separation on a ZIF-8 membrane. This somewhat underestimates the measured ethene/ethane mixture separation factor of 2.4 for an equimolar mixture at 6 bar (cf. Fig. 2). The derivation might be – at least partially – due to the highly simplified model, based on the Fick's first law assuming a constant diffusion coefficient and a linear concentration gradient. While assuming a linear concentration gradient might be appropriate, the diffusion coefficients however highly depend on loading (Fig. 5). It should be noted that the diffusion selectivity of ZIF-8 can be obtained as well exclusively by simulations as shown for ZIF-8 in comparison to the 8-ring window zeolites LTA, CHA, DDR [32] (Fig. 6).

In Fig. 7, some approximations are shown which account for the loading dependency of the diffusion coefficients in a rather simple way. Approach 1 refers to the above mentioned calculation method of choosing diffusion coefficient on the feed side of the membrane. In approach 2, we used the averaged loading at the feed and permeate side to determine the diffusion coefficient. While approach 1 leads to a slight underestimation, approach 2 slightly overestimates

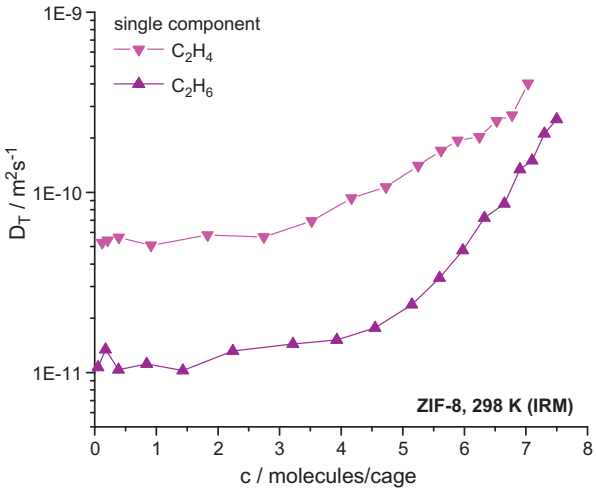

Fig. 6. Transport diffusion coefficients D_T at $T = 298$ K as derived from sorption uptake experiments of the single gases ethene and ethane on a large ZIF-8 single crystal as shown in Fig. 3 with IRM detection. The relationship between loading and gas pressure follows from Fig. 4. Calibration of the IRM by GCMC.

the separation factor at higher loadings. For both approaches, the reason for the deviation is the sudden increase in the ethane and ethane diffusivities at a loading of around four C_2 molecules/cage. In contrast, the ethene/ethane adsorption ratio (adsorption selectivity) remains almost constant over the whole pressure range. For approach 1, this leads to a rapid drop in ethene/ethane separation factor, since the diffusivity of ethane increases somewhat faster with increasing loading as the diffusivity of ethene. The averaged concentration, used in approach 2, stays below the concentration of four C_2 molecules/cage and, hence, does not include the diffusivity increase at this concentration. This approach predicts a nearly constant separation factor. Apparently, both approximations fail in describing the real situation accurately. In a third approach, the averaged diffusion selectivity calculated from the diffusion selectivity at the feed and permeate side is used, which seems to fit quite good with the experiment. Although the decrease in diffusion selectivity on the feed side at high pressure is included, due to the

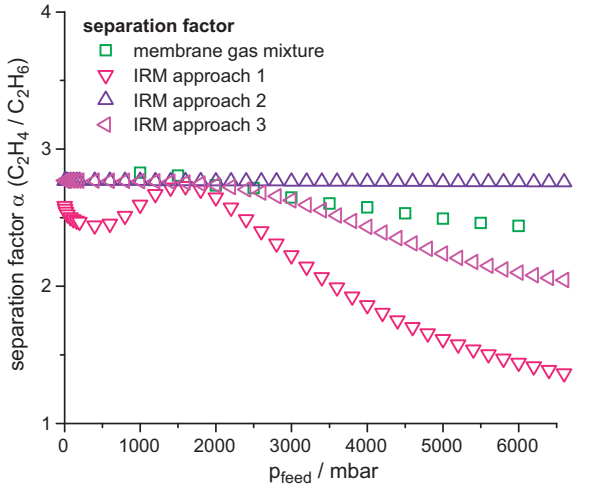

Fig. 7. Comparison of different simple approaches accounting in the loading dependency of the diffusion coefficient. Approach 1 is calculated using the diffusion coefficients D_T derived from the loading on the feed side of the ZIF-8 membrane. In approach 2, the averaged loadings across the membrane were used to determine the diffusion coefficients. For approach 3, an averaged selectivity was calculated by forming the ratio of the feed side selectivity (high loadings) and the permeate side selectivity (low loadings).

averaging with the constant diffusion selectivity of the permeate side, the drop in separation factor it is less rapid. This well working approach of a diffusivity at the average concentration similar to the one of Crank [24], who suggested to use an average diffusivity over the relevant range of concentration.

In addition to the interpretation and correlation of the mixture behavior so far discussed in this paper, the single component permeances can be predicted with sufficient accuracy from the GCMC-IRM single gas adsorption and diffusion data. In single gas permeation, ethene and ethane fluxes of 1.24 ml cm^{-2} min^{-1} and 0.29 ml cm^{-2} min^{-1} have been measured at room temperature for pressure differences of 5 bar (6 bar on the feed and 1 bar on the permeate side). Following Fick's first law with $j_i = -D_i\, grad\, c_i$ the fluxes j_i of ethene and ethane through the membrane can be roughly estimated from the single gas GCMC-IRM data and compared with the above permeation measurements. The concentration gradient $grad\, c_i$ is approximated by the concentration difference Δc_i between the loadings of the ZIF-8 on the feed side at 6 bar and on the permeate side at 1 bar divided by the membrane thickness of 25 μm and assuming a u.c. volume of 4905.3 $Å^3$ [20] or 4900 $Å^3$ [33].

From Fig. 4, the concentration differences Δc_i between the ethene and ethane loading under aforementioned conditions are 4.2 and 2.9 molecules/cage,[2] respectively. Assuming an average loading of 4.6 molecules ethene/cage and 5.7 molecules ethane/cage, pure component diffusivities D_i of 1×10^{-10} m^2 s^{-1} for ethene and 3.9×10^{-11} m^2 s^{-1} for ethane are obtained from the loading dependency of diffusivity in Fig. 6. With this approximation, we estimate an ethene flux of 1.70 ml cm^{-2} min^{-1} and an ethane flux of 0.46 ml cm^{-2} min^{-1} which are near to the measured data.

This quite consistent picture of C_2 adsorption and diffusion in ZIF-8 single crystals and through membranes derived from membrane permeation, IRM adsorption/desorption and GCMC calculations is rather surprising. Similar correlations for zeolite membranes but using much more qualified models predicted much higher membrane fluxes than really measured e.g. using the Maxwell–Stefan-based models for silicalite-1 membranes [34,35] and for DDR membranes [36]. One reason for the fact that our simple approach works well might be that the ZIF-8 membrane layer shown in Fig. 1 consists of larger crystals with a low contribution of mass transport via grain boundaries in comparison with zeolite membranes. From the time and space resolved concentration profiles (not shown here) it can be concluded that sorption uptake/desorption is controlled by intracrystalline diffusion rather than by a surface transport resistance caused by an amorphous surface layer as it was found for Zn(tbip) – as a less stable MOF structure towards chemical degradation in comparison to ZIF-8 [37,38]. In another recent study on large FAU "single" crystals it was found that internal twin planes running through the crystal can reduce the translational mobility [39].

4. Conclusions

Membrane selectivities can be predicted with sufficient accuracy as the product of adsorption and diffusion selectivity. Both can be obtained from sorption uptake experiments on large single crystals by IR microscopy. We demonstrated this procedure for the ethene separation from an equimolar ethene/ethane mixture for different feed pressures at room temperature. At 6 bar feed pressure, the product of the ethene/ethane adsorption selectivity (0.5) and diffusion selectivity (2.7) gives an estimated permeation selectivity of 1.4 which is near to the measured ethene/ethane selectivity of 2.4. We ascribe this underestimation mainly to the assumption

[2] u.c. corresponds to 2 cages (cf. [20,33]).

of constant diffusion coefficients in the simple model. However, using averaged loading to determine diffusion coefficients or by calculating the averaged selectivity of feed and permeate side, the underestimation could be compensated. Furthermore, based on the diffusion coefficients and loadings derived from sorption uptake studies with IR detection, the single gas fluxes of ethene and ethane could be predicted with sufficient accuracy following Fick's first law. The good agreement might indicate that in the case of ZIF-8 inner transport barriers, like crystal defects and grain boundaries, as well as outer barriers like surface resistances, only slightly influence the macroscopic mass transport through the membrane. The preferential ethene diffusion competes with the preferential ethane adsorption thus reducing the ethene selectivity of the ZIF-8 membrane. The phenomena of opposed diffusion and adsorption selectivities might however be resolved by the very unique hybrid organic–inorganic character of ZIFs or MOFs in general. Functionalization of linker molecules – even post-synthesis [40] – might allow controlling interactions with olefins to improve the ethene/ethane adsorption selectivity of ZIFs.

Acknowledgements

This work is part of the DFG Priority Program SPP 1362 "Porous Metal–Organic Frameworks", organized by S. Kaskel. The financial support is gratefully acknowledged.

References

[1] J.-R. Li, R.J. Kuppler, H.-C. Zhou, Selective gas adsorption and separation in metal–organic frameworks, Chem. Soc. Rev. 38 (2009) 1477–1504.
[2] K. Li, D.H. Olson, J. Seidel, T.J. Emge, H. Gong, H. Zeng, J. Li, Zeolitic imidazolate frameworks for kinetic separation of propane and propene, J. Am. Chem. Soc. 131 (2009) 10368–10369.
[3] M. Hartmann, S. Kunz, D. Himsl, O. Tangermann, S. Ernst, A. Wagner, Adsorptive separation of isobutene and isobutane on $Cu_3(BTC)_2$, Langmuir 24 (2008) 8634–8642.
[4] M. Maes, L. Alaerts, F. Vermoortele, R. Ameloot, S. Couck, V. Finsy, J.F.M. Denayer, D.E. De Vos, Separation of C_5-hydrocarbons on microporous materials: complementary performance of MOFs and zeolites, J. Am. Chem. Soc. 132 (2010) 2284–2292.
[5] H. Guo, G. Zhu, I.J. Hewitt, S. Qiu, "Twin copper source" growth of metal–organic framework membrane: $Cu_3(BTC)_2$ with high permeability and selectivity for recycling H_2, J. Am. Chem. Soc. 131 (2009) 1646–1647.
[6] R. Ranjan, M. Tsapatsis, Microporous metal organic framework membrane on porous support using the seeded growth method, Chem. Mater. 21 (2009) 4920–4924.
[7] Y. Liu, E. Hu, E.A. Khan, Z. Lai, Synthesis and characterization of ZIF-69 membranes and separation for CO_2/CO mixture, J. Membr. Sci. 353 (2010) 36–40.
[8] S.R. Venna, M.A. Carreon, Highly permeable zeolite imidazolate framework-8 membranes for CO_2/CH_4 separation, J. Am. Chem. Soc. 132 (2010) 76–78.
[9] J. Gascon, F. Kapteijn, Metal–organic framework membranes-high potential, bright future? Angew. Chem. Int. Ed. 49 (2010) 1530–1532.
[10] M.C. McCarthy, V. Varela-Guerrero, G.V. Barnett, H.-K. Jeong, Synthesis of zeolitic imidazolate framework films and membranes with controlled microstructures, Langmuir 26 (2010) 14636–14641.
[11] V.V. Guerrero, Y. Yoo, M.C. McCarthy, H.-K. Jeong, J. Mater. Chem. 20 (2010) 3938–3943.
[12] A. Huang, W. Dou, J. Caro, Steam-stable zeolitic imidazolate framework ZIF-90 membrane with hydrogen selectivity through covalent functionalization, J. Am. Chem. Soc. 132 (2010) 15562–15564.
[13] Y. Li, F. Liang, H. Bux, A. Feldhoff, W. Yang, J. Caro, Molecular sieve membrane: supported metal–organic framework with high hydrogen selectivity, Angew. Chem. Int. Ed. 49 (2010) 548–551.
[14] Y. Li, F. Liang, H. Bux, W. Yang, J. Caro, Zeolitic imidazolate framework ZIF-7 based molecular sieve membrane for hydrogen separation, J. Membr. Sci. 354 (2010) 48–54.
[15] Y.-S. Li, H. Bux, A. Feldhoff, G.-L. Li, W.-S. Yang, J. Caro, Controllable synthesis of metal–organic frameworks: from MOF nanorods to oriented MOF membranes, Adv. Mater. 22 (2010) 3322–3326.
[16] H. Bux, F. Liang, Y. Li, J. Cravillon, M. Wiebcke, J. Caro, Zeolitic imidazolate framework membrane with molecular sieve properties by microwave assisted solvothermal growth, J. Am. Chem. Soc. 131 (2009) 16000–16001.
[17] A. Huang, H. Bux, F. Steinbach, J. Caro, Molecular sieve membrane with hydrogen permselectivity: ZIF-22 in LTA topology prepared with 3-aminopropyltriethoxysilane as covalent linker, Angew. Chem. Int. Ed. 49 (2010) 4958–4961.
[18] S. Keskin, D.S. Sholl, Progress, Opportunities, and challenges for applying atomically detailed modeling to molecular adsorption and transport in metal–organic framework materials, Ind. Eng. Chem. Res. 48 (2009) 2355–2371.
[19] E. Haldoupis, S. Nair, D.S. Sholl, Efficient calculation of diffusion limitations in metal organic framework materials: a tool for identifying materials for kinetic separations, J. Am. Chem. Soc. 132 (2010) 7528–7539.
[20] H. Bux, C. Chmelik, J.M. van Baten, R. Krishna, J. Caro, Novel MOF-membrane for molecular sieving predicted by IR-diffusion studies and molecular modeling, Adv. Mater. 22 (2010) 4741–4743.
[21] C. Chmelik, H. Bux, J. Caro, L. Heinke, F. Hibbe, T. Titze, J. Kärger, Mass transfer in a nanoscale material enhanced by an opposite flux, Phys. Rev. Lett. 104 (2010) 085902.
[22] R. Krishna, Describing the diffusion of guest molecules inside porous structures, J. Phys. Chem. C 113 (2009) 19756–19781.
[23] W.J. Koros, Y.H. Ma, T. Shimidzu, Terminology for membranes and membrane processes, Pure Appl. Chem. 68 (1996) 1479–1489.
[24] J. Crank, The Mathematics of Diffusion, Oxford University Press, 1980, ISBN: 10:0198534116.
[25] R. Krishna, J.M. van Baten, In silico screening of zeolite membranes for CO_2 capture, J. Membr. Sci. 360 (2010) 323–333.
[26] R. Krishna, J.M. van Baten, Using molecular simulations for screening of zeolites for separation of CO_2/CH_4 mixtures, Chem. Eng. J. 133 (2007) 121–131.
[27] R. Krishna, J.M. van Baten, Screening of zeolite adsorbents for separation of hexane isomers: a molecular simulation study, Sep. Purif. Technol. 55 (2007) 246–255.
[28] A.L. Myers, J.M. Prausnitz, Thermodynamics of mixed-gas adsorption, AIChE J. 11 (1965) 121–127.
[29] D.D. Do, H.D. Do, Cooperative and competitive adsorption of ethylene, ethane, nitrogen and argon on graphitized carbon black and in slit pores, Adsorption 11 (2005) 35–50.
[30] M.C. Kroon, L.F. Vega, Selective paraffin removal from ethane/ethylene mixtures by adsorption into aluminum methylphosphonate-α: a molecular simulation study, Langmuir 25 (2009) 2148–2152.
[31] D.H. Olsen, M.A. Camblor, L.A. Villaescusa, G.H. Kuehl, Light hydrocarbon sorption properties of pure silica SI-CHA and ITQ-3 and high silica ZSM-58, Micropor. Mesopor. Mater. 67 (2004) 27–33.
[32] R. Krishna, J.M. Van Baten, A molecular dynamics investigation of the diffusion characteristics of cavity-type zeolites with 8-ring windows, Micropor. Mesopor. Mater. 137 (2011) 83–91.
[33] S.A. Moggach, T.D. Benett, A.K. Cheetham, The effect of pressure on ZIF-8: increasing pore size with pressure and the formation of a high-pressure phase at 1.47 GPa, Angew. Chem. Int. Ed. 48 (2009) 7087–7089.
[34] J.M. van de Graaf, F. Kapteijn, J.A. Moulijn, Modeling permeation of binary mixtures through zeolite membranes, AIChE J. 45 (1999) 497–511.
[35] J.M. van de Graaf, F. Kapteijn, J.A. Moulijn, Permeation of weakly adsorbing components through a silicalite-1 membrane, Chem. Eng. Sci. 54 (1999) 1081–1092.
[36] J. van den Bergh, M. Mittelmaijer-Hazeleger, F. Kapteijn, Modeling permeation of CO_2/CH_4, N_2/CH_4 and CO_2/air mixtures across a DD3R zeolite membrane, J. Phys. Chem. C 114 (2010) 9379–9389.
[37] C. Chmelik, F. Hibbe, D. Tzoulaki, L. Heinke, J. Caro, J. Li, J. Kärger, Exploring the nature of surface barriers on MOF Zn(tbip) by applying IR microscopy in high temporal and spatial resolution, Micropor. Mesopor. Mater. 129 (2010) 340–344.
[38] D. Tzoulaki, L. Heinke, H. Lim., J. Li, D. Olson, J. Caro, R. Krishna, C. Chmelik, Assessing surface permeabilities from transient guest profiles in nanoporous host materials, Angew. Chem. Int. Ed. 48 (2009) 3525–3528.
[39] A. Feldhoff, J. Caro, H. Jobic, J. Olivier, C.B. Krause, P. Galvosas, J. Kärger, Intracrystalline transport resistances in nanoporous zeolite X crystals, PhysChemPhys 10 (2009) 2429–2433.
[40] W. Morris, C.J. Doonan, H. Furuikawa, R. Banerjee, O.M. Yaghi, Crystals as molecules: postsynthesis covalent functionalization of zeolitic imidazolate frameworks, J. Am. Chem. Soc. 130 (2008) 12626–12627.
[41] C. Gücüyener, J. van den Bergh, J. Gascon, F. Kapteijn, Ethane/Ethene separation turned on its head: Selective ethane adsorption on the metal-organic framework ZIF-7 through a gate-opening mechanism, J. Am. Chem. Soc. 132 (2010) 17704–17706.